Suyehiro, K., Sacks, I.S., Acton, G.D., and Oda, M. (Eds.)
Proceedings of the Ocean Drilling Program, Scientific Results Volume 186

8. Composite Depth Scales for the Japan Trench, ODP Leg 186 Sites 1150 and 1151[1]

Jennifer C. McGuire[2] and Gary D. Acton[3]

ABSTRACT

We present composite depth scales for the multiply cored intervals from Sites 1150 and 1151. These new depth scales place coeval strata recovered in cores from different holes at a single site into a common stratigraphic framework. At Site 1150, double coring between Holes 1150A and 1150B occurred over only a short interval between ~703 and 713 meters below seafloor (mbsf), but this is sufficient to tie the upper portion of the stratigraphic section cored in Hole 1150A to the lower portion cored in Hole 1150B. The upper ~100 m of the sedimentary section at Site 1151 was double cored with the advanced piston corer and partially cored with the rotary core barrel, resulting in the complete recovery of this interval. The composite depth scales were constructed using Splicer software to vertically adjust the relative depths of various cores from one hole to the depths from another hole so as to align distinct physical properties measured on cores. The magnetic susceptibility data was the physical property most easily correlated between holes, and therefore primarily used to create a composite depth scale and spliced stratigraphic section. The spliced section is a continuous stratigraphic section constructed from representative cored intervals from the holes at a site. Both the splice and the composite depth scale can be applied to other data sets from Site 1151 to provide a stratigraphically continuous and laterally consistent basis for interpreting lithologic features or data sets. The resulting composite scale showed a 30% improvement in correlation of the magnetic susceptibility data relative to the original mbsf depth scale, and comparable improvement when applied to the other data sets.

[1]McGuire, J.C., and Acton, G.D., 2003. Composite depth scales for the Japan Trench, ODP Leg 186 Sites 1150 and 1151. *In* Suyehiro, K., Sacks, I.S., Acton, G.D., and Oda, M. (Eds.), *Proc. ODP, Sci. Results,* 186, 1–23 [Online]. Available from World Wide Web: <http://www-odp.tamu.edu/publications/186_SR/VOLUME/CHAPTERS/102.PDF>. [Cited YYYY-MM-DD]
[2]Department of Geology and Geophysics, Texas A&M University, College Station TX 77843-3115, USA.
[3]Ocean Drilling Program, 1000 Discovery Drive, College Station TX 77845-9547, USA. Correspondence author: **acton@odpemail.tamu.edu**

Initial receipt: 10 August 2001
Acceptance: 12 August 2002
Web publication: 28 February 2003
Ms 186SR-102

INTRODUCTION

During Ocean Drilling Program (ODP) Leg 186, two sites (Sites 1150 and 1151) were drilled in the deep-sea terrace west of the Japan Trench (Fig. F1) (Sacks, Suyehiro, Acton, et al., 2000). At each site, middle Miocene to Holocene sedimentary sections were recovered that were over a kilometer thick. Sedimentation rates vary between 20 and 248 m/m.y. over the entire section, but average ~119 m/m.y. at Site 1150 and ~103 m/m.y. at Site 1151 over the Brunhes normal polarity interval (0–0.78 Ma). A sedimentary record spanning the past 1 m.y. is thus preserved in the upper 100 m of the section, in which multiple holes have been cored. These multiply cored intervals, particularly those at Site 1151, are the primary focus of this study.

The sediments are very homogeneous, consisting mostly of diatomaceous clays and oozes interbedded with thin volcanic ash layers. Although the sites are part of an accretionary wedge along an active subduction zone, the upper 300 m of sediment sustained little or no visual deformation. The upper portions of the sedimentary sections at these sites thus have the potential to provide a wealth of information about the paleoceanographic, geologic, and volcanic history of the region.

As is typical for a single drill hole, coring gaps and intervals affected by coring disturbances result in incomplete recovery of the sedimentary section. Thus, ODP has adopted a strategy of coring multiple holes at a site to ensure complete or nearly complete recovery of a continuous sedimentary record. During Leg 186, this strategy was employed at Site 1151 but only after the primary objective of installing a geophysical observatory had been successfully completed. Because of time constraints, Hole 1151A was cored with the rotary core barrel (RCB) system to a depth of 1113.6 meters below seafloor (mbsf) to determine lithologic changes that are important for establishing casing depths (Table T1). As part of this, the upper 78 m of the section were washed away during a jet-in test (Shipboard Scientific Party, 2000c). The geophysical instrument package was then installed in Hole 1151B, where no cores were recovered. With time remaining, the upper portion of the sedimentary section at Holes 1151C and 1151D were cored with the advanced piston corer (APC) to 97.2 and 93.0 mbsf, respectively. In addition, to ensure stratigraphic overlap and optimize recovery between Holes 1150A and 1150B, a short interval at ~720 mbsf was double cored. In this study, we place the multiply cored intervals at each site into a common stratigraphic framework by conducting between-hole correlation and establishing a common or composite depth scale.

A composite depth scale (measured in meters composite depth, or mcd) places coeval, laterally continuous stratigraphic features into a common frame of reference by shifting the mbsf depth scales of individual cores to maximize correlation between holes (e.g., Hagelberg et al., 1995; Acton et al., 2001). By definition, the individual cores are shifted vertically, without permitting expansion or contraction of the relative depth scale within any core. In essence, the composite depth scale overcomes many of the inadequacies of the mbsf depth scale, which is based on drill pipe measurements and is unique to each hole. By ODP convention, the drill pipe measurement defines the depth to the top of each core.

Deviations of mbsf depths from true depths arise from errors and uncertainties in depth measurements, most of which can be attributed to

F1. ODP Leg 186 location map, p. 10.

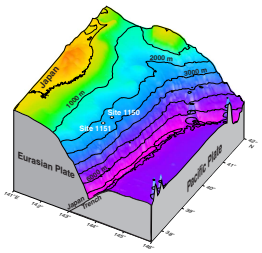

T1. Composite depth scale, Site 1151, p. 20.

ship motion, in addition to core expansion, incomplete recovery, and tides. Therefore a horizontal feature present in recovered material from several holes, which in the absence of local bathymetric variations should have the same true depth, will likely have different mbsf depths (Fig. F2). Errors in the mbsf depth scale range from a few centimeters to several meters, though rarely more than ~10 m (e.g., Acton et al., 2001, and references therein). After establishing an mcd scale, more complete stratigraphic records are spliced from the data from multiple holes.

The primary goals of this study are to establish common depth scales and spliced stratigraphic records for (1) the three holes at Site 1151 and (2) the two holes at Site 1150. Commonly, this type of work is completed during an ODP cruise. This was not possible during Leg 186 because a stratigraphic correlator had not been staffed for the leg and insufficient time was available between the completion of coring in Holes 1151C and 1151D and the end of Leg 186. Below, we present the data used to construct the mcd scales and outline the methods to achieve accurate between-hole correlations.

F2. Natural log of the magnetic susceptibility in the mbsf depth scale, Holes 1151A, 1151C, and 1151D, p. 11.

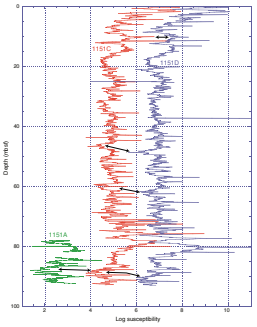

DATA

The primary data sets we used were (1) the whole-core magnetic susceptibility, (2) color reflectance component data (lightness, L*, and chromaticity parameters, a* and b*) (Balsam et al., 1997; Blum, 1997; Balsam et al., 1998; Balsam and Damuth, 2000) from split-core working-half sections, and (3) the magnetic intensity from the split-core archive-half sections following alternating field (AF) demagnetization at 20 mT (Sacks, Suyehiro, Acton, et al., 2000). These three data sets were collected during Leg 186 using the multisensor track (MST), the Minolta color scanner, and the long-core cryogenic magnetometer, respectively (Shipboard Scientific Party, 2000a). Core photographs and core descriptions of various intervals (Sacks, Suyehiro, Acton, et al., 2000) provided additional constraints for the correlations, and were used to detect intervals disturbed by drilling. Magnetic susceptibility records provided the highest overall degree of correlation throughout the holes, as well as the highest sampling resolution. The susceptibility values are presented as raw meter values, which can be converted to SI volume susceptibility units by multiplying by ~0.7×10^{-5} (Blum, 1997). The cores were sampled at 2-cm intervals for susceptibility and 5-cm intervals for other data sets. Additionally, magnetic susceptibility or intensity data collected within 5 cm of the end of each section or from intervals that were disturbed by the drilling and recovery process were removed before making correlations for the mcd scale. This includes gaps caused by the removal of 5-cm-long interstitial water (IW) samples, which are taken from the ends of some sections prior to MST and other measurements. This "gap or disturbance" record is recorded in Table T2. The most common disturbed intervals visible from the photographic records were the top 5–70 cm of each core, which frequently contains water-saturated sediments. Other disturbed intervals identified in the data record are gas voids or sediments deformed by "suck-in" or other forms of severe core deformation.

T2. Intervals disturbed or distorted by coring or whole-round sample collection, p. 21.

The magnetic susceptibility and magnetic intensity data were converted to natural logarithm format to avoid the preferential correlation of exceptionally large peaks within the data set. Correlations were then made primarily using the log-susceptibility and log-intensity data from each hole. The magnetic intensity data were used to refine the correla-

tions when correlation of the magnetic susceptibility data was ambiguous or difficult. Reflectance data were also compared between holes. In general, the reflectance data were difficult to correlate independently, but marked improvement in correlation was visible when the mcd scale derived using the other data sets was applied to the reflectance data.

ANALYSIS AND RESULTS

The mcd scale was constructed using the program Splicer (version 2.2, available on the World Wide Web from the Borehole Research Group at the Lamont-Doherty Earth Observatory of Columbia University at **www.ldeo.columbia.edu/BRG/ODP**). Splicer allows data sets from several holes at a given site to be uploaded and correlated simultaneously. Only one data set is shown in Splicer's main viewing window at a time. Multiple data sets can be loaded in a single session, however, and the user can switch among them in the main window. Correlations are first made visually by selecting a tie point from data in one hole and comparing it directly with data from another hole at the same site. Ties determined from the physical or magnetic properties data are intended to correlate matching data patterns and amplitudes. Distinct stratigraphic features, such as many of the volcanic ash layers, can also be correlated between holes (Fig. **F3**). Matching characteristics of these layers, such as their descriptions recorded in the visual core descriptions or spikes in the magnetic susceptibility data, assist in correlation of continuous individual ash layers over the region. Table **T3** lists the correlations made for ash layers at Site 1151.

Importing multiple data sets into Splicer allows the cross-correlation coefficients for all data sets to be computed simultaneously for the given composite depth scale. Depth adjustments that provide the best correlation within a preferred data set or a compromise of correlation coefficients among all the data sets are chosen. The values of the cross-correlation coefficient vary from +1 to –1. A value of +1 indicates perfect correlation (such as would be obtained by comparing identical data sets), values near zero indicate poor or no correlation, and a value of –1 indicates anticorrelation (such as would be obtained by comparing a data set to its inverse). Each time a depth adjustment is made within Splicer, the coefficient is recalculated, allowing the user to determine the preferred correlation. The window over which the coefficient is calculated is adjustable. The default window length of ±2.00 m on either side of the selected tie point was used for most correlations. This window was reduced to ±1.00 m as needed to focus on specific features or to avoid anomalous features such as those biased by coring disturbances.

Correlation begins by selecting the core that has the most pristine record of the upper portion of the upper few meters of the sedimentary record, particularly the mudline (sediment/water interface). This first core is defined as the top of the composite section, and its mcd is the same as its mbsf depth. At Site 1151, the top of the composite section is Core 186-1151D-1H. A tie point that gives the preferred correlation is selected between data from this core and a core in a second hole. All the data from the second hole below the correlation point are vertically shifted to align the tie points between the holes. Once the appropriate tie is determined and the depth adjustment made, the shifted section becomes part of the reference section. The process continues downhole, vertically shifting the data one core at a time, relative to data from the

F3. Interbedded volcanic ash layers, p. 12.

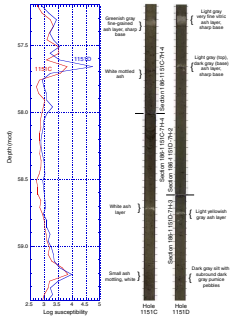

T3. Correlation of ash layers, Site 1151, p. 22.

other hole. By tying points of different mbsf depths, Splicer vertically adjusts the individual sections of core and brings the chosen features into the common mcd scale. The tie points are added to the Splicer "affine" table, which records all the depth adjustments that define the composite depth scale, in units of mcd. The depths to the top of each core (obtained in mbsf format from the ODP Janus database) are given in Table **T1,** and converted from mbsf to mcd scales using the offsets calculated in Splicer and recorded in the affine table.

No expansion or compression of the depth scale within a core or core interval is permitted within Splicer. Due to this restriction, it is not possible to correlate every feature exactly with features in other holes. In some intervals, relative expansion of sediments from one core to another was apparent. In these cases, the correlation was determined using the tie that visually minimized offset over the interval and showed the best overall graphical representation of the correlation coefficients.

In addition to the obvious visual improvement in correlation of data between holes by using the mcd rather than the mbsf scale, the overall improvement is quantified by using the program Analyseries (Paillard et al., 1996). The magnetic susceptibility data sets for Holes 1151C and 1151D were imported into Analyseries to determine an initial linear correlation coefficient between the data sets from 0 to 96 mbsf. Points of the same mbsf depth at the top and bottom in each data set were tied, and a linear correlation coefficient between 1 and –1 was obtained. The same data in the mcd scale, determined using Splicer, were then imported to Analyseries at various stages in the correlation process to provide a quantitative assessment of incremental improvement in correlation of the composite depth scale relative to the mbsf depth scale. In cases where the preferred correlation was ambiguous in Splicer, depth shifts that improved the overall linear correlation in Analyseries were retained in the composite depth scale, and those that degraded the correlation were discarded. The overall linear correlation coefficient for the magnetic susceptibility data for Holes 1151C and 1151D in the mbsf scale prior to any depth shifting was 0.650. After using Splicer to create a composite depth scale, the overall linear correlation coefficient improved to 0.845.

Additional constraints will become available as new data sets are acquired, such as U-channel paleomagnetic measurements and tephrachronology studies. The composite depth scale constructed already shows good correlation of ash layers (Table **T3**) between holes, and tephrachronology could confirm these correlations. Similarly, the composite depth scale results in excellent agreement in magnetostratigraphic constraints between Holes 1151C and 1151D. Specifically, the Brunhes/Matuyama boundary occurs at 82.26 mcd for both holes, even though this boundary was not used as a constraint in constructing the composite depth scale. In general, coeval features agree to better than ~10 cm as noted with the ash layers (Table **T3**), even though differences of ~20 cm are observed and can be expected given the resolution of the data used to construct the composite depth scale.

The data sets for Holes 1151A, 1151C, and 1151D were spliced to create a continuous downhole sedimentary section for Site 1151 (Figs. **F4, F5, F6**). The spliced record is a continuous stratigraphic section constructed from representative portions (or intervals) of data from the available holes at a site. The splice was created using the magnetic susceptibility data, but the tie points (Table **T4**) can be applied to the other data sets. Because the splice is optimized for susceptibility, gaps or artificial steps can occur in other data sets as shown in Figure **F5.** The splice

F4. Natural log of the magnetic susceptibility in the mcd scale, Holes 1151A, 1151C, 1151D, and the Site 1151 splice record, p. 13.

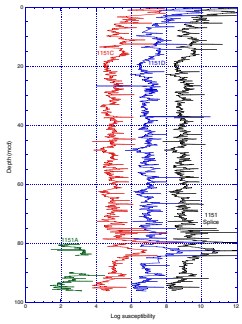

F5. Natural log of the magnetic intensity in the mcd scale, Holes 1151A, 1151C, 1151D, and the Site 1151 splice record, p. 14.

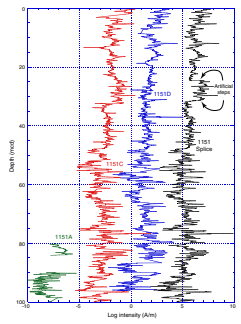

F6. The a* reflectance data, p. 15.

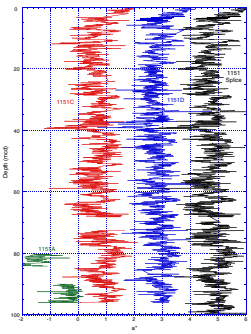

T4. Splice tie points, Site 1151, p. 23.

is nonunique in that some intervals may be equally represented by more than one of the holes drilled at the site. When selecting tie points for the spliced record, as much data from a single core as possible was kept intact, minimizing the number of alternations between holes needed to provide the total spliced record. The exception to this approach was in intervals that contained large data spikes. Placing the tie points in these areas was avoided to reduce creating artificial steps within the spliced susceptibility data set.

Site 1150 provided only minimal overlap of cored intervals with recovery only from Holes 1150A and 1150B. Hole 1150A was cored to 713.00 mbsf (78.38% recovery) and Hole 1150B was cored continuously from 703.30 to 1172.00 mbsf (56.30% recovery), providing potential overlap only between 703.30 and 713.00 mbsf (Fig. F7). Within this narrow interval, only two depth shifts were required to align Hole 1150B to Hole 1150A. In both cases, Hole 1150B was shifted to align with Hole 1150A. As a result, the mbsf and mcd scales are identical for Hole 1150A. In Hole 1150B, Core 186-1150B-1R should be shifted 0.18 m downward, and all cores from Core 186-1150B-2R and below should be shifted 1.02 m downward from the originally recorded mbsf depths to place them within the mcd scale. Within the overlap interval, correlation of Holes 1150A and 1150B give a correlation coefficient of –0.125 in the mbsf scale. The slight adjustments made in the overlap region improve the correlation coefficient to 0.210 in the mcd scale. The overall correlation for Site 1150 is still poor, however, both in visual and mathematical terms. A spliced data set was not constructed for Site 1150, as the minimal degree of overlap would leave most of the data set essentially unchanged from the original sequence.

F7. Natural log of the magnetic susceptibility, Holes 1150A and 1150B, p. 16.

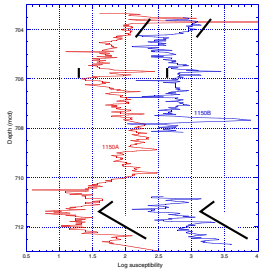

DISCUSSION AND CONCLUSIONS

The mcd scale is expanded relative to the mbsf scale in all holes at Site 1151 by varying amounts (Fig. F8). Hole 1151A showed the greatest expansion, increasing by 7.0% from the original mbsf length over the upper 93.3 m cored. The mcd scale was 5.9% longer than the mbsf scale for Hole 1151C, and 3.7% longer in Hole 1151D. Differences in drill types between Hole 1151A and Holes 1151C and 1151D, as well as difficulties in the measurements of mbsf depths as described below, are likely causes of the differences in scales. These results are consistent with the mcd scales developed at other sites, which reported lengthening of the mcd scale relative to the mbsf scale by about 10% (e.g., Alexandrovich and Hays, 1989; Farrell and Janecek, 1991; Hagelberg et al., 1995; MacKillop et al., 1995; Lyle, Koizumi, Richter, et al., 1997; Acton et al., 2001).

F8. Depth vs. offsets, p. 17.

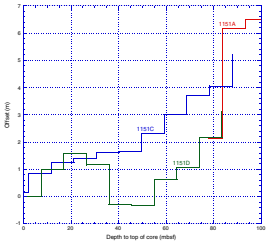

Drilling and recovery procedures are potential sources of the differences in depths to lithologic boundaries observed among different holes (Ruddiman et al., 1987; Ruddiman, Kidd, Thomas, et al., 1987; Ruddiman, Sarnthein, Baldauf, et al., 1988; Alexandrovich and Hays, 1989; Murray and Prell, 1991; Farrell and Janecek, 1991; Harris et al., 1995; Lyle, Koizumi, Richter, et al., 1997). For example, the release of overburden pressure upon recovery of a core causes expansion of the sediments. Heave and drift of the ship may result in inaccurate estimation of the drill string length, as well as result in repeat coring of some sections of the hole, causing further error in mbsf depth measurements. The cohesiveness of the sediments, affected by such factors as the water content, may also contribute to the expansion of a core. Small-scale

faulting or slumping within a hole during coring may result in further core expansion and recovery that exceeds 100%.

It should be kept in mind that the composite depth scale is a first-order correlation in which the length scales of individual cores are not expanded or contracted. Because relative expansion occurs between coeval intervals, correlative features may be misaligned by a few tens of centimeters or less. For the log magnetic intensity data in Figure **F9**, for example, the distinct peaks at ~69 mcd in Holes 1151C and 1151D are tied, but this causes an observable offset in the data immediately above and below this correlation. Figure **F10** shows another example in the magnetic susceptibility data, with data in Hole 1151D between 8.5 and 12.8 mcd expanded relative to the coeval interval in Hole 1151C. Although it is possible this mismatch reflects lateral variation in sedimentation rates, it is more likely a result of relative core expansion given the short distance between holes. This trade-off in matching some features at the expense of the misalignment of other features within the coeval interval is repeated throughout the data sets. By relaxing the constraint that a core's length scale be fixed, higher-order correlations can be made that would permit the alignment of features on the order of a centimeter or better. Studies that require correlation of features at this scale can be achieved using Analyseries or methods such as those outlined by Martinson et al. (1982). The first-order correlations presented here yield an ~30% improvement in the correlation coefficients between holes and establish an important depth template for building higher-order scales.

F9. Depth correlation tie made along the double peak, p. 18.

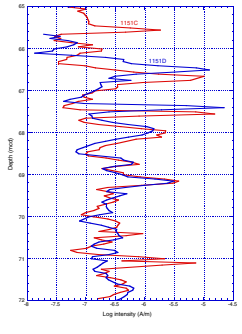

F10. Slight misalignment of correlative features, p. 19.

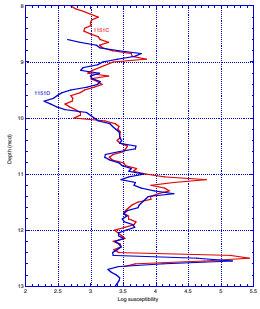

ACKNOWLEDGMENTS

We thank the reviewers (David Mallinson and Sara Harris) and ODP editor (Heather Nevill) for their assistance. This research used samples and/or data provided by the Ocean Drilling Program (ODP). ODP is sponsored by the U.S. National Science Foundation (NSF) and participating countries under management of Joint Oceanographic Institutions (JOI), Inc. Funding for this research was provided by a JOI/USSSP (United States Science Support Program) grant to G. Acton.

REFERENCES

Acton, G.D., Borton, C.J., and the Leg 178 Shipboard Scientific Party, 2001. Palmer Deep composite depth scales for Leg 178 Sites 1098 and 1099. *In* Barker, P.F., Camerlenghi, A., Acton, G.D., and Ramsay, A.T.S. (Eds.), *Proc. ODP, Sci. Results,* 178 [Online]. Available from World Wide Web: <http://www-odp.tamu.edu/publications/178_SR/chap_05/chap_05.htm>. [Cited 2002-07-23]

Alexandrovich, J.M., and Hays, J.D., 1989. High-resolution stratigraphic correlation of ODP Leg 111 Holes 677A and 677B and DSDP Leg 69 Hole 504. *In* Becker, K., Sakai, H., et al., *Proc. ODP, Sci. Results,* 111: College Station, TX (Ocean Drilling Program), 263–276.

Balsam, W.L., and Damuth, J.E., 2000. Further investigations of shipboard vs. shore-based spectral data: implications for interpreting Leg 164 sediment composition. *In* Paull, C.K., Matsumoto, R., Wallace, P., and Dillon, W.P. (Eds.), *Proc. ODP, Sci. Results,* 164: College Station, TX (Ocean Drilling Program), 313–324.

Balsam, W.L., Damuth, J.E., and Schneider, R.R., 1997. Comparison of shipboard vs. shore-based spectral data from Amazon-Fan Cores: implications for interpreting sediment composition. *In* Flood, R.D., Piper, D.J.W., Klaus, A., and Peterson, L.C. (Eds.), *Proc. ODP, Sci. Results,* 155: College Station, TX (Ocean Drilling Program), 193–215.

Balsam, W.L., Deaton, B.C., and Damuth, J.E., 1998. The effects of water content on diffuse reflectance measurements of deep-sea core samples: an example from ODP Leg 164 sediments. *Mar. Geol.,* 149:177–189.

Blum, P., 1997. Physical properties handbook: a guide to the shipboard measurement of physical properties of deep-sea cores. *ODP Tech. Note,* 26 [Online]. Available from World Wide Web: <http://www-odp.tamu.edu/publications/tnotes/tn26/INDEX.HTM>. [Cited 2002-07-23]

Farrell, J.W., and Janecek, T.R., 1991. Late Neogene paleoceanography and paleoclimatology of the northeast Indian Ocean (Site 758). *In* Weissel, J., Peirce, J., Taylor, E., Alt, J., et al., *Proc. ODP, Sci. Results,* 121: College Station, TX (Ocean Drilling Program), 297–355.

Hagelberg, T.K., Pisias, N.G., Shackleton, N.J., Mix, A.C., and Harris, S., 1995. Refinement of a high-resolution, continuous sedimentary section for studying equatorial Pacific Ocean paleoceanography, Leg 138. *In* Pisias, N.G., Mayer, L.A., Janecek, T.R., Palmer-Julson, A., and van Andel, T.H. (Eds.), *Proc. ODP, Sci Results,* 138: College Station, TX (Ocean Drilling Program), 31–46.

Harris, S., Hagelberg, T., Mix, A., Pisias, N.G., and Shackleton, N.J., 1995. Sediment depths determined by comparisons of GRAPE and logging density data during Leg 138. *In* Pisias, N.G., Mayer, L.A., Janecek, T.R., Palmer-Julson, A., and van Andel, T.H. (Eds.), *Proc. ODP, Sci. Results,* 138: College Station, TX (Ocean Drilling Program), 47–57.

Lyle, M., Koizumi, I., Richter, C., et al., 1997. *Proc. ODP, Init. Repts.,* 167: College Station, TX (Ocean Drilling Program).

MacKillop, A.K., Moran, K., Jarrett, K., Farrell, J., and Murray, D., 1995. Consolidation properties of equatorial Pacific Ocean sediments and their relationship to stress history and offsets in the Leg 138 composite depth sections. *In* Pisias, N.G., Mayer, L.A., Janecek, T.R., Palmer-Julson, A., and van Andel, T.H. (Eds.), *Proc. ODP, Sci. Results,* 138: College Station, TX (Ocean Drilling Program), 357–369.

Martinson, D.G., Menke, W., and Stoffa, P.L., 1982. An inverse approach to signal correlation. *J. Geophys. Res.,* 87:4807–4818.

Murray, D.W., and Prell, W.L., 1991. Pliocene to Pleistocene variations in calcium carbonate, organic carbon, and opal on the Owen Ridge, northern Arabian Sea. *In* Prell, W.L., Niitsuma, N., et al., *Proc. ODP, Sci. Results,* 117: College Station, TX (Ocean Drilling Program), 343–363.

Paillard, D., Labeyrie, L., and Yiou, P., 1996. Macintosh program performs time-series analysis. *Eos,* 77:379.

Ruddiman, W., Sarnthein, M., Baldauf, J., et al., 1988. *Proc. ODP, Init. Repts.,* 108 (Sections 1 and 2): College Station, TX (Ocean Drilling Program).

Ruddiman, W.F., Cameron, D., and Clement, B.M., 1987. Sediment disturbance and correlation of offset holes drilled with the hydraulic piston corer: Leg 94. *In* Ruddiman, W.F., Kidd, R.B., Thomas, E., et al., *Init. Repts. DSDP,* 94 (Pt. 2): Washington (U.S. Govt. Printing Office), 615–634.

Ruddiman, W.F., Kidd, R.B., Thomas, E., et al., 1987. *Init. Repts. DSDP,* 94 (Pts. 1 and 2): Washington (U.S. Govt. Printing Office).

Sacks, I.S., Suyehiro, K., Acton, G.D., et al., 2000. *Proc. ODP, Init. Repts.,* 186 [CD-ROM]. Available from: Ocean Drilling Program, Texas A&M University, College Station TX 77845-9547, USA.

Shipboard Scientific Party, 2000a. Explanatory notes. *In* Sacks, I.S., Suyehiro, K., Acton, G.D., et al., *Proc. ODP, Init. Repts.,* 186, 1–51 [CD-ROM]. Available from: Ocean Drilling Program, Texas A&M University, College Station TX 77845-9547, USA.

————, 2000b. Leg 186 summary. *In* Sacks, I.S., Suyehiro, K., Acton, G.D., et al., *Proc. ODP, Init. Repts.,* 186, 1–37 [CD-ROM]. Available from: Ocean Drilling Program, Texas A&M University, College Station TX 77845-9547, USA.

————, 2000c. Site 1151. *In* Sacks, I.S., Suyehiro, K., Acton, G.D., et al., *Proc. ODP, Init. Repts.,* 186, 1–125 [CD-ROM]. Available from: Ocean Drilling Program, Texas A&M University, College Station TX 77845-9547, USA.

Figure F1. ODP Leg 186 location map (Shipboard Scientific Party, 2000b).

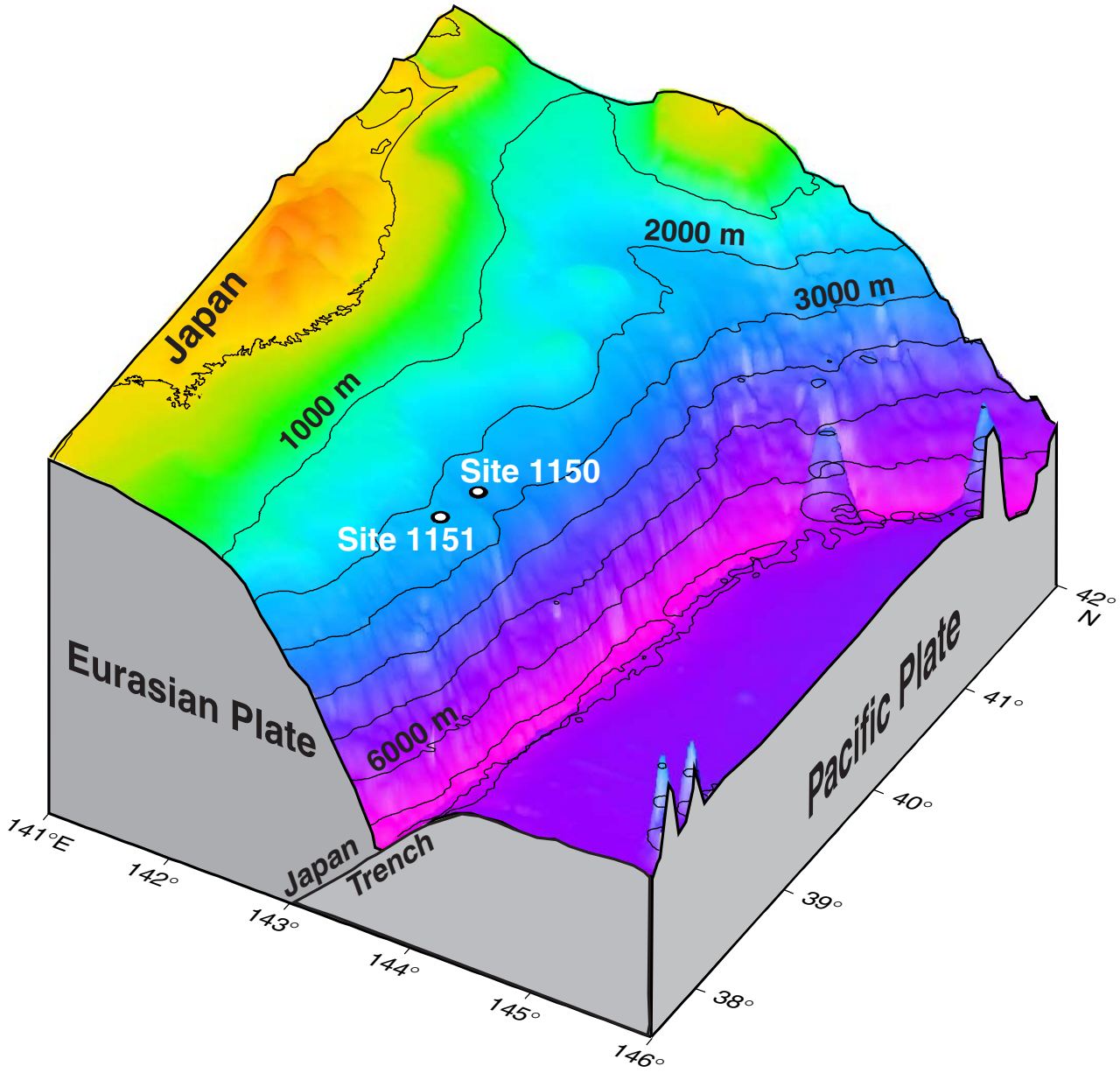

Figure F2. The natural log of the magnetic susceptibility (raw meter units) for Holes 1151A (bold green), 1151C (red), and 1151D (blue) in the mbsf depth scale. Integer values of +2 and +4 were added to each data point for Holes 1151C and 1151D, respectively, to separate data for purposes of display. The mbsf depth offset is obvious between several distinctive correlative data patterns (arrows).

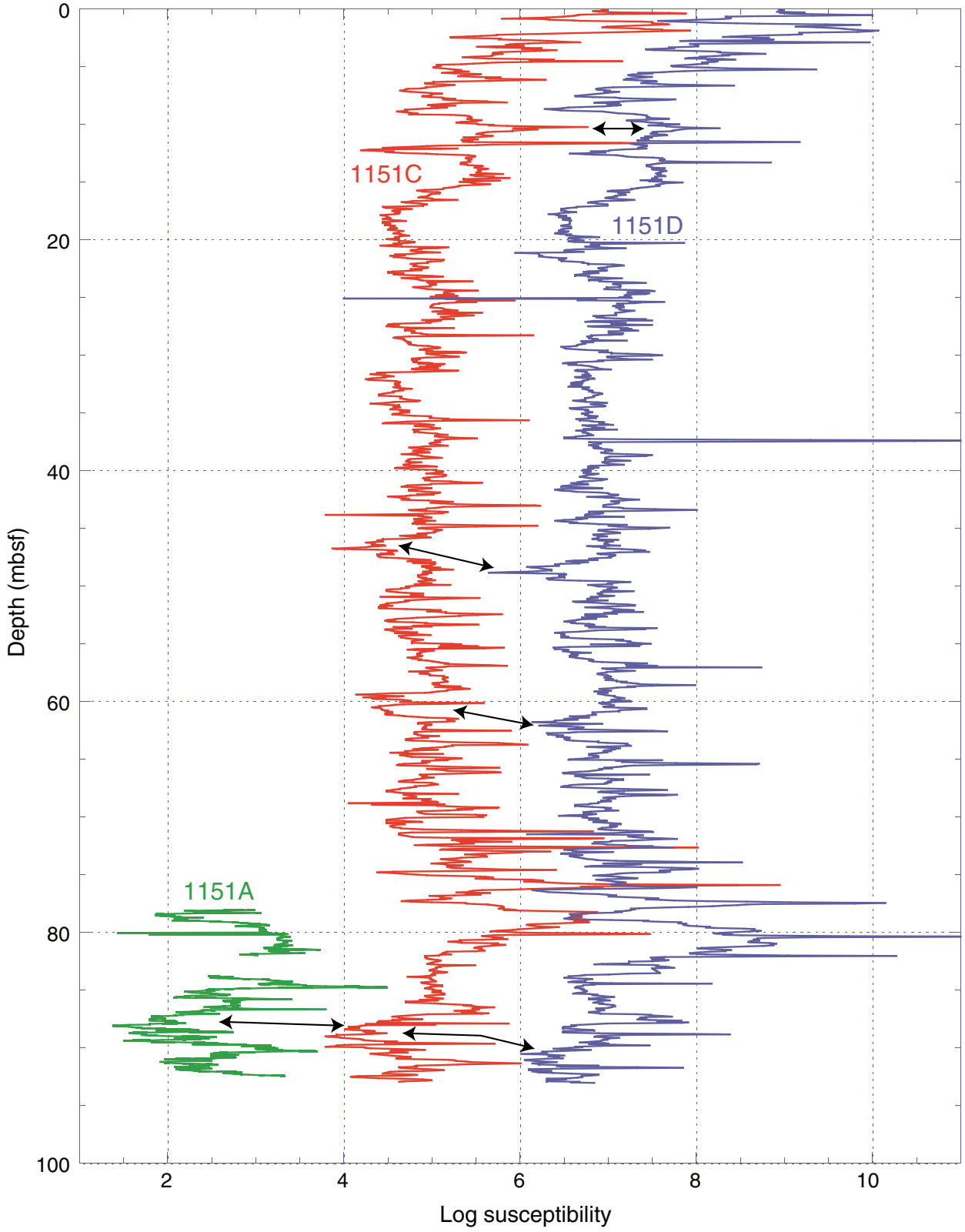

Figure F3. Core photographs from intervals 186-1151C-7H-4, 69 cm, to 7H-5, 139 cm, and 186-1151D-7H-2, 9 cm, to 7H-3, 79 cm, showing multiple interbedded volcanic ash layers in a largely homogeneous matrix consisting of diatomaceous clays and oozes. Descriptions next to core photographs are from the visual core descriptions (Shipboard Scientific Party, 2000c). White mottled ash and pumice are difficult to see in core photographs but are visible in cores as noted.

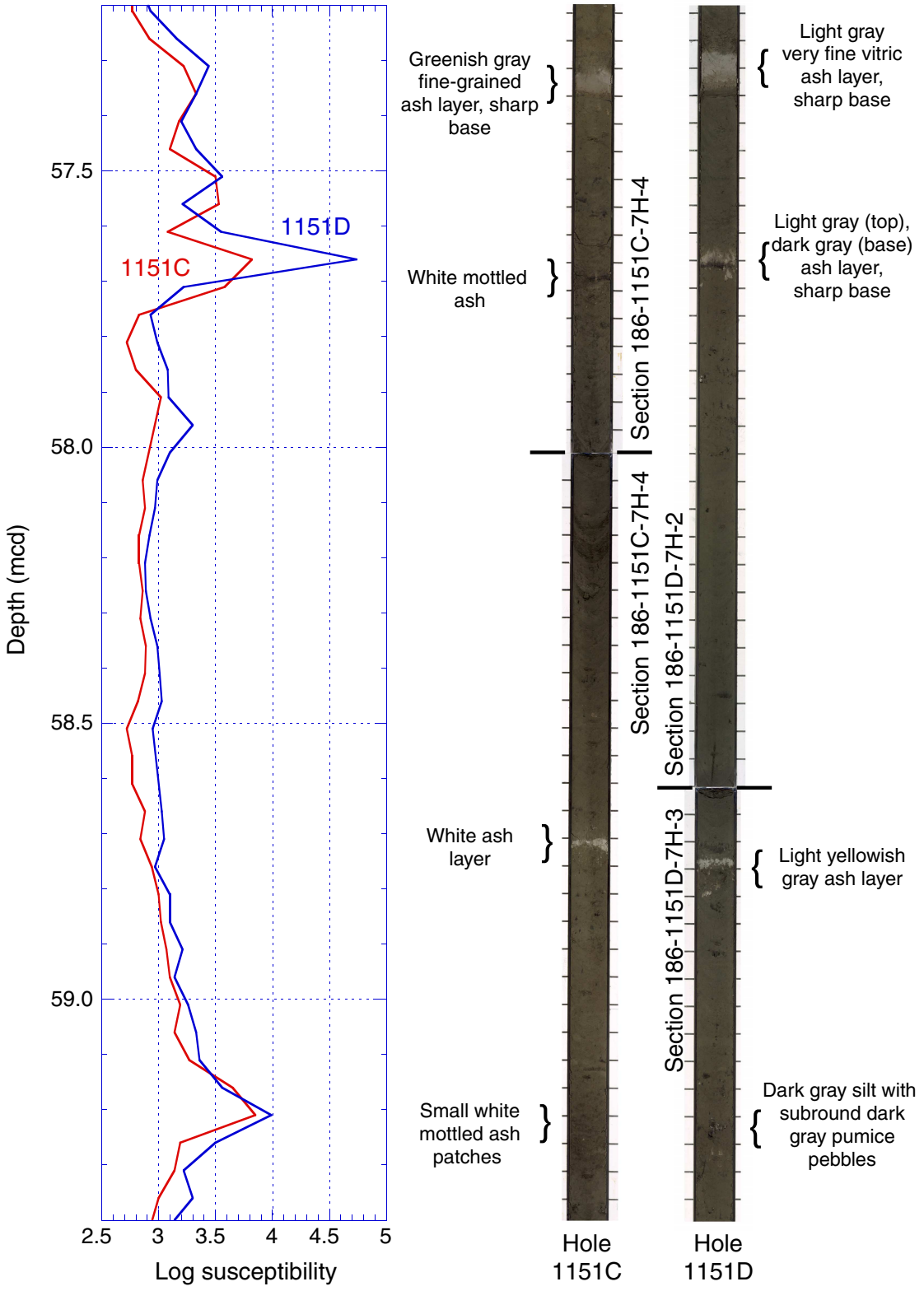

Figure F4. The natural log of the magnetic susceptibility (raw meter units) for Holes 1151A (bold green), 1151C (red), 1151D (blue), and the Site 1151 splice record (black) in the mcd scale. Integer values of +2, +4, and +6 were added to each data point from Holes 1151C and 1151D and for the spliced record, respectively, to separate data for the purposes of display. The depth correlation between data is visibly improved using the mcd scale as noted by comparison to Figure F2, p. 11.

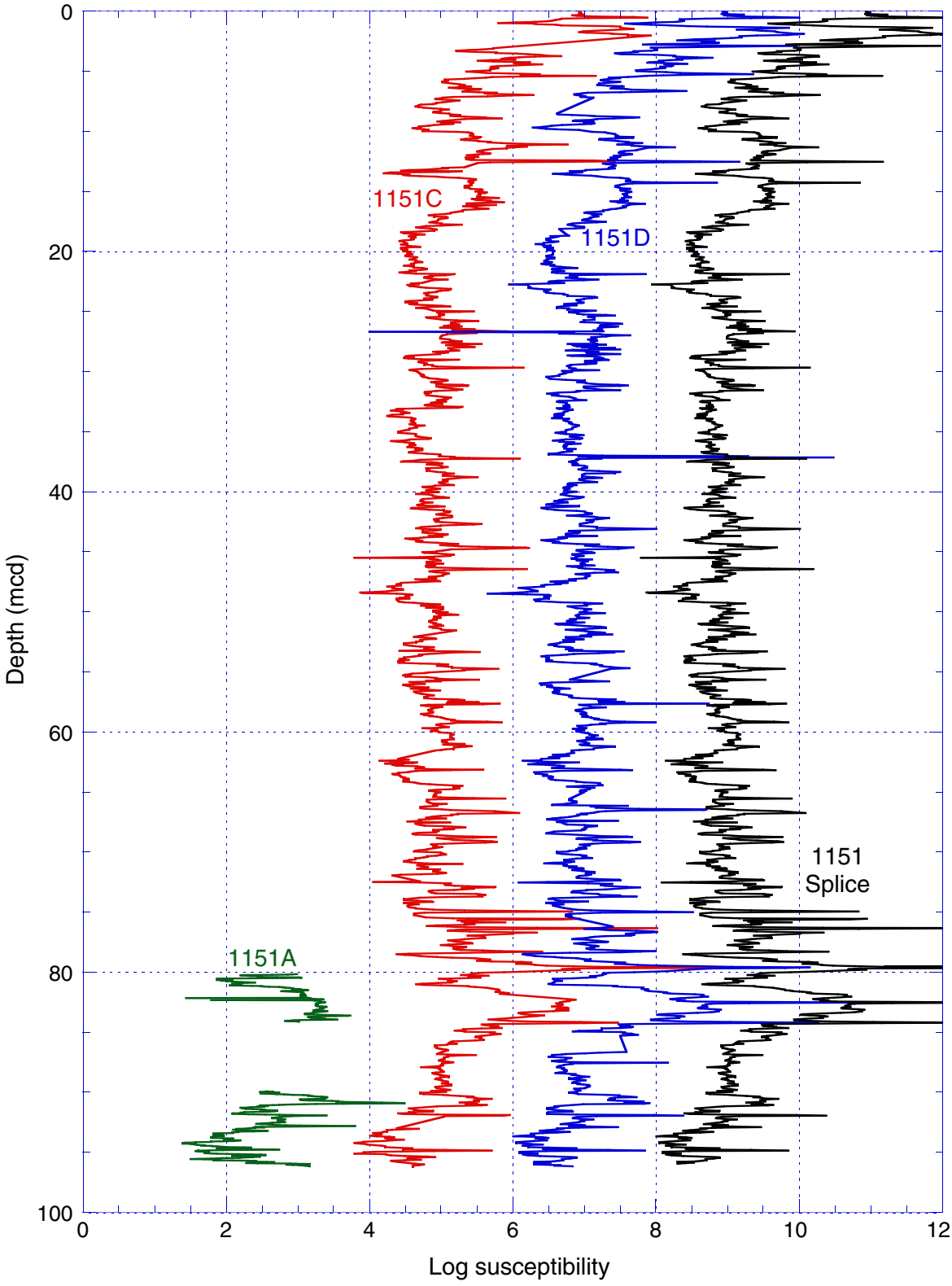

Figure F5. The natural log of the magnetic intensity (after 20-mT AF demagnetization) for Holes 1151A (bold green), 1151C (red), 1151D (blue), and the Site 1151 splice record (black) in the mcd scale. Integer values of +4, +8, and +12 were added to each data point from Holes 1151C and 1151D and for the spliced record, respectively, to separate data for the purposes of display. The artificial steps in the spliced intensity record occur because the spliced intervals were constructed using the magnetic susceptibility data.

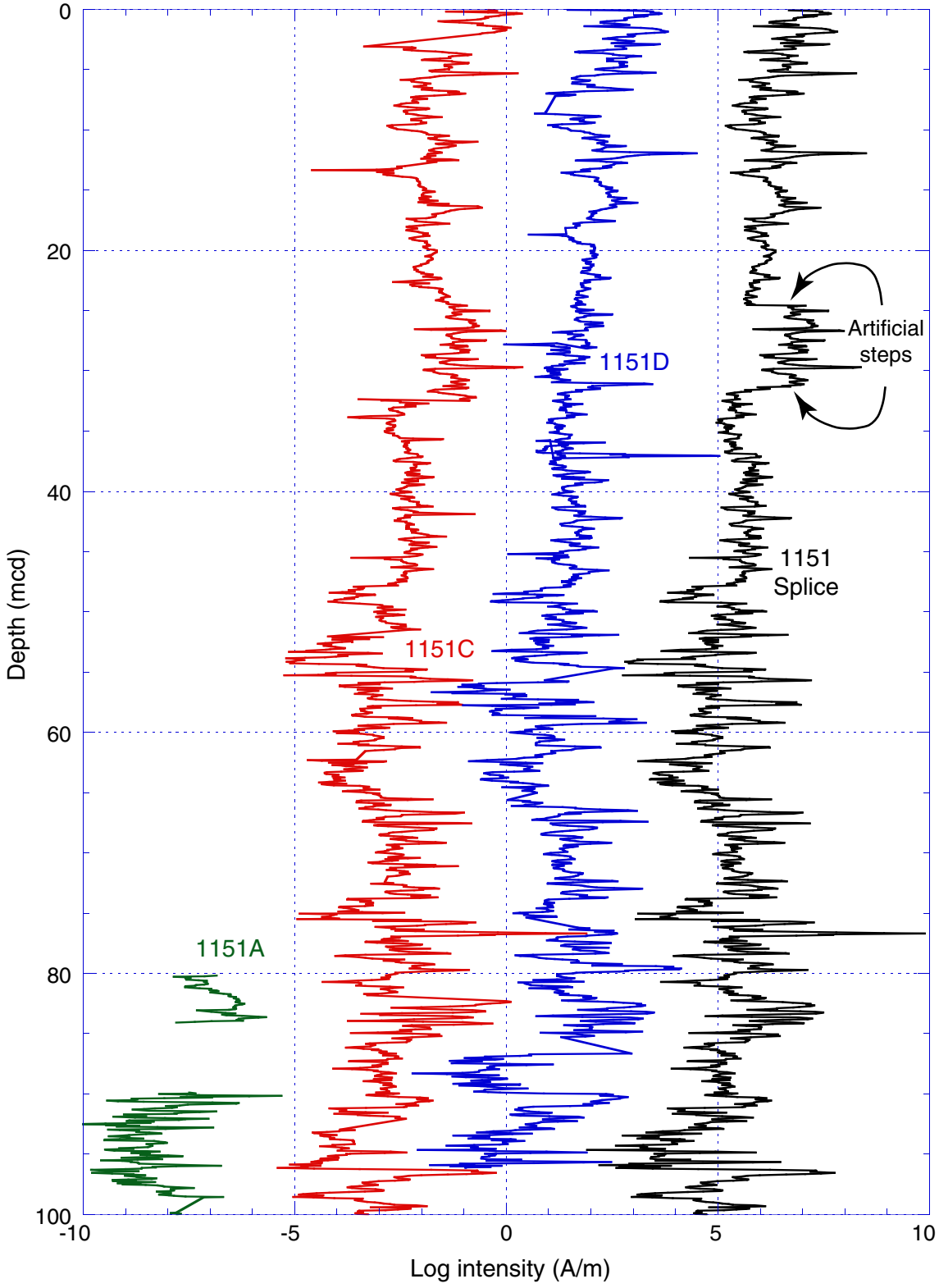

Figure F6. The a* reflectance data for Holes 1151A (bold green), 1151C (red), and 1151D (blue) in the mcd scale. Integer values of +1 and +2 were added to each data point from Holes 1151C and 1151D, respectively, to separate data for purposes of display.

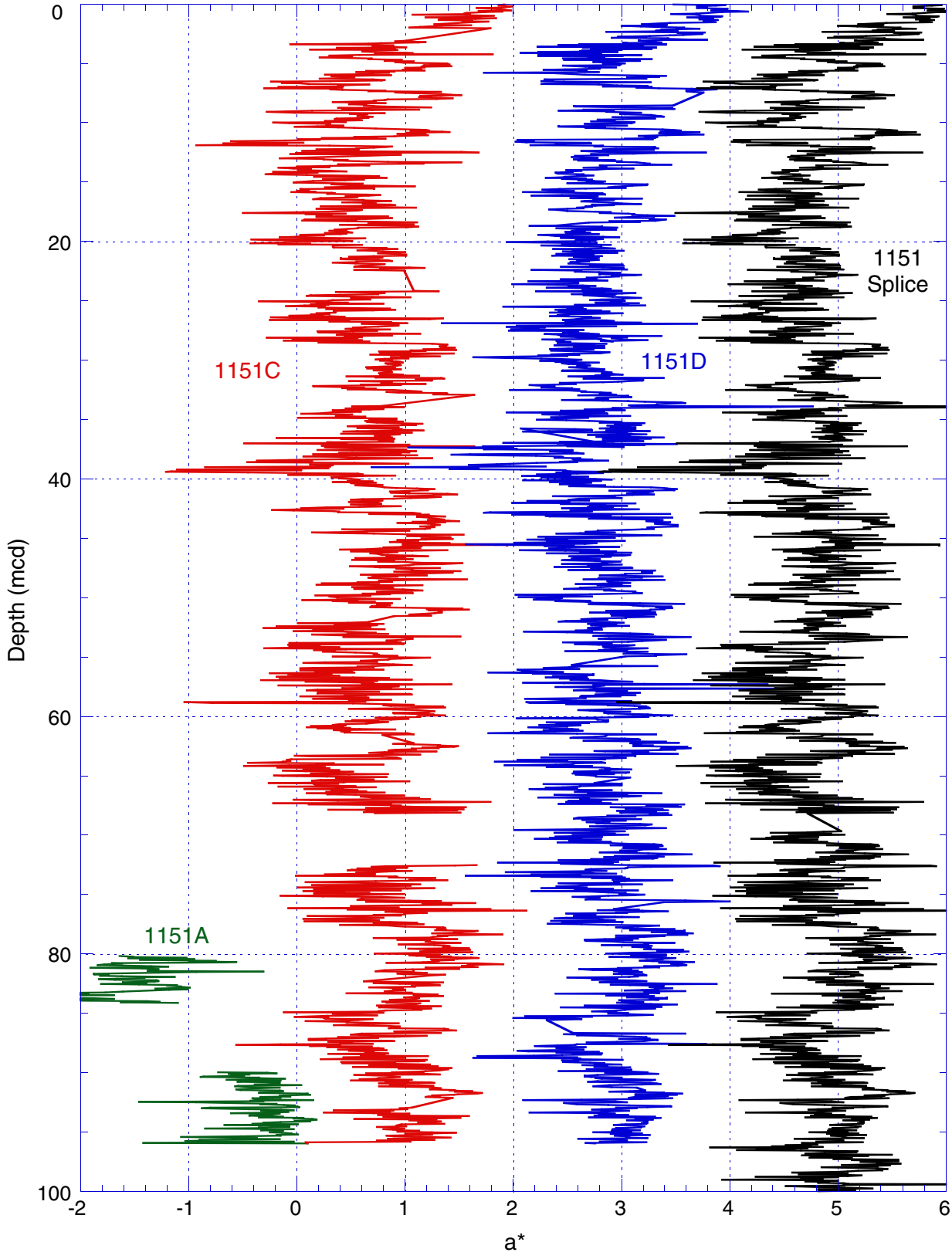

Figure F7. The natural log of the magnetic susceptibility (raw meter units) for Holes 1150A (red) and 1150B (blue). Integer values of +1 were added to each data point from Hole 1150B to separate data for purposes of display. Correlations were made only in the region of overlapping recovery, from 703.30 to 713.00 mbsf. Correlative features are denoted with thick black lines.

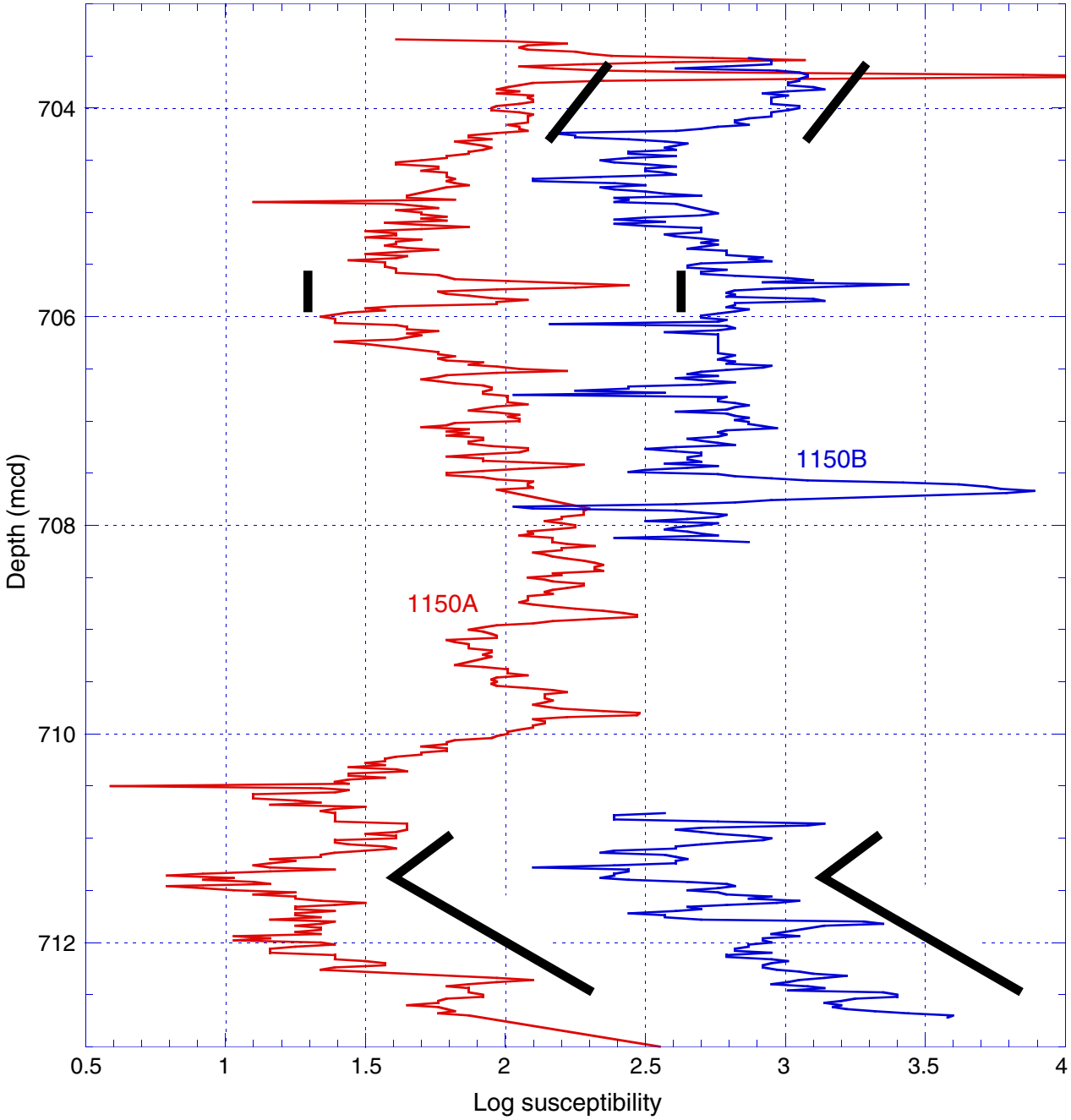

Figure F8. Depth (in mbsf) vs. the offsets (in meters) needed to place cores from Holes 1151A (red), 1151C (blue), and 1151D (green) into the mcd scale.

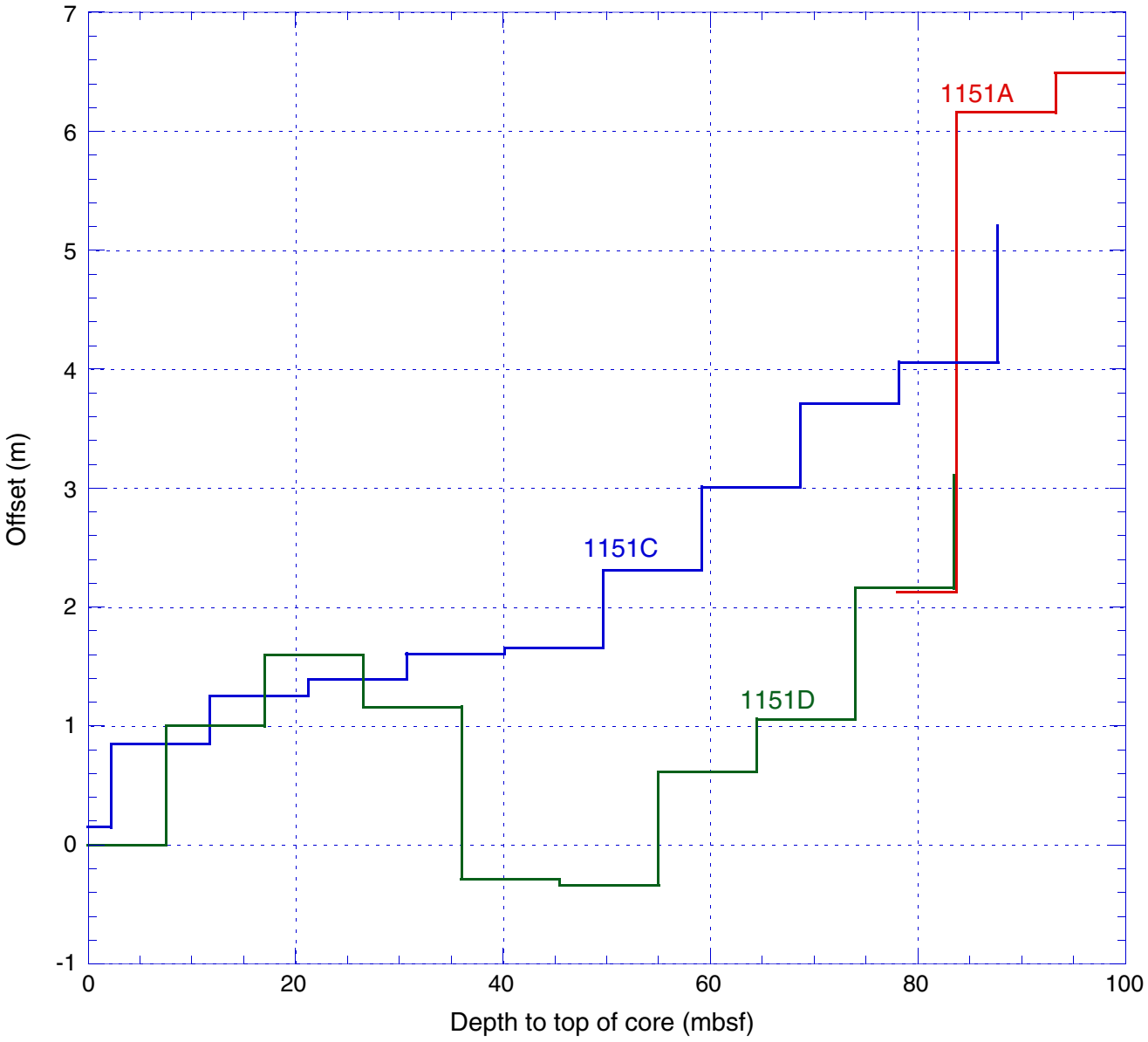

Figure F9. The natural log of the magnetic intensity (after 20-mT AF demagnetization) from Holes 1151C (red) and 1151D (blue) plotted to show depth correlation tie made along the double peak at ~69 mcd. Expansion or contraction of data in Hole 1151D relative to Hole 1151C is indicated by misalignment of correlative peaks above and below this tie point.

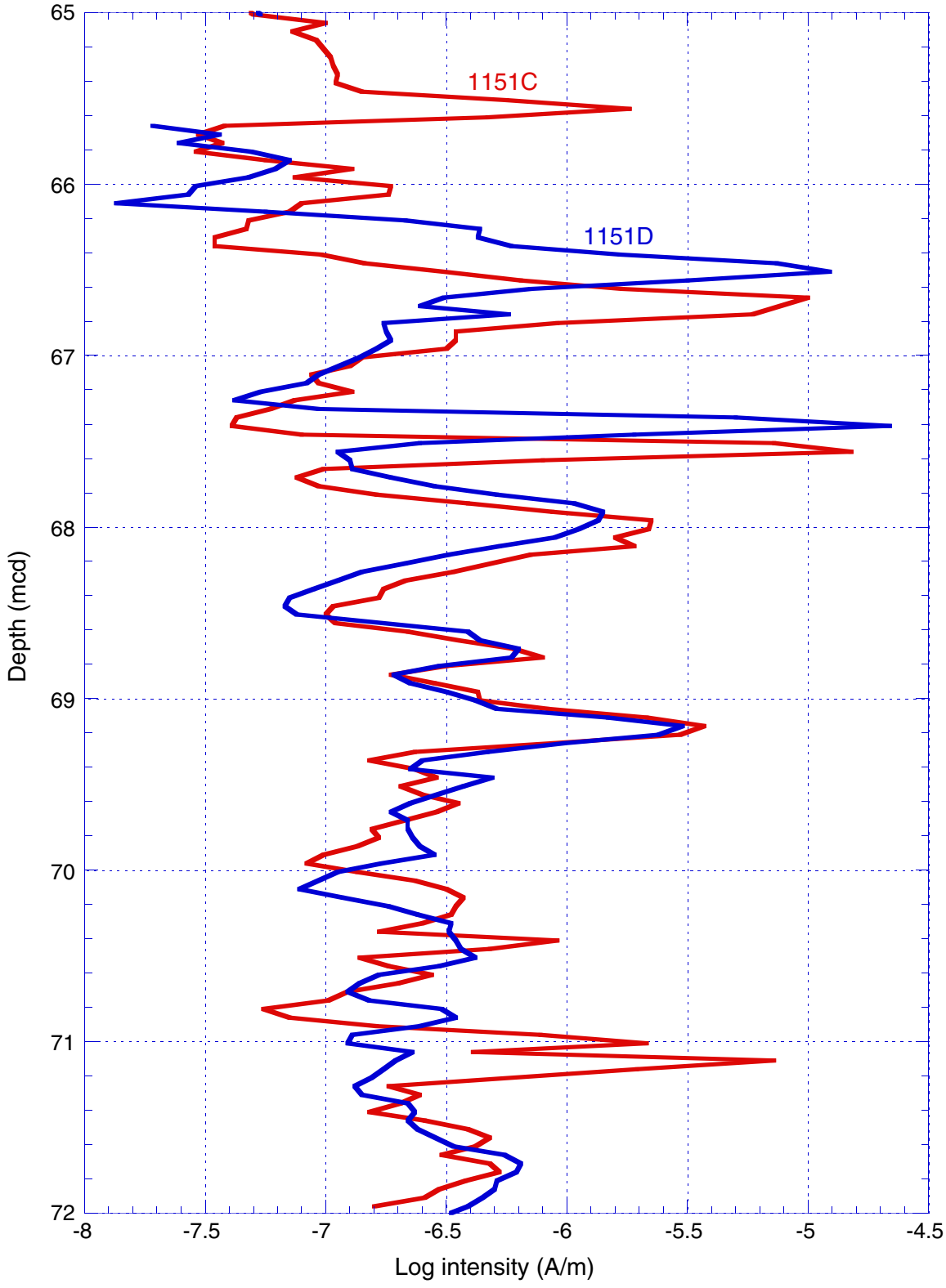

Figure F10. The natural log of the magnetic susceptibility (raw meter units) from Holes 1151C (red) and 1151D (blue), overlain to show slight misalignment of correlative features that occur above and below ~10.3–11.0 mcd.

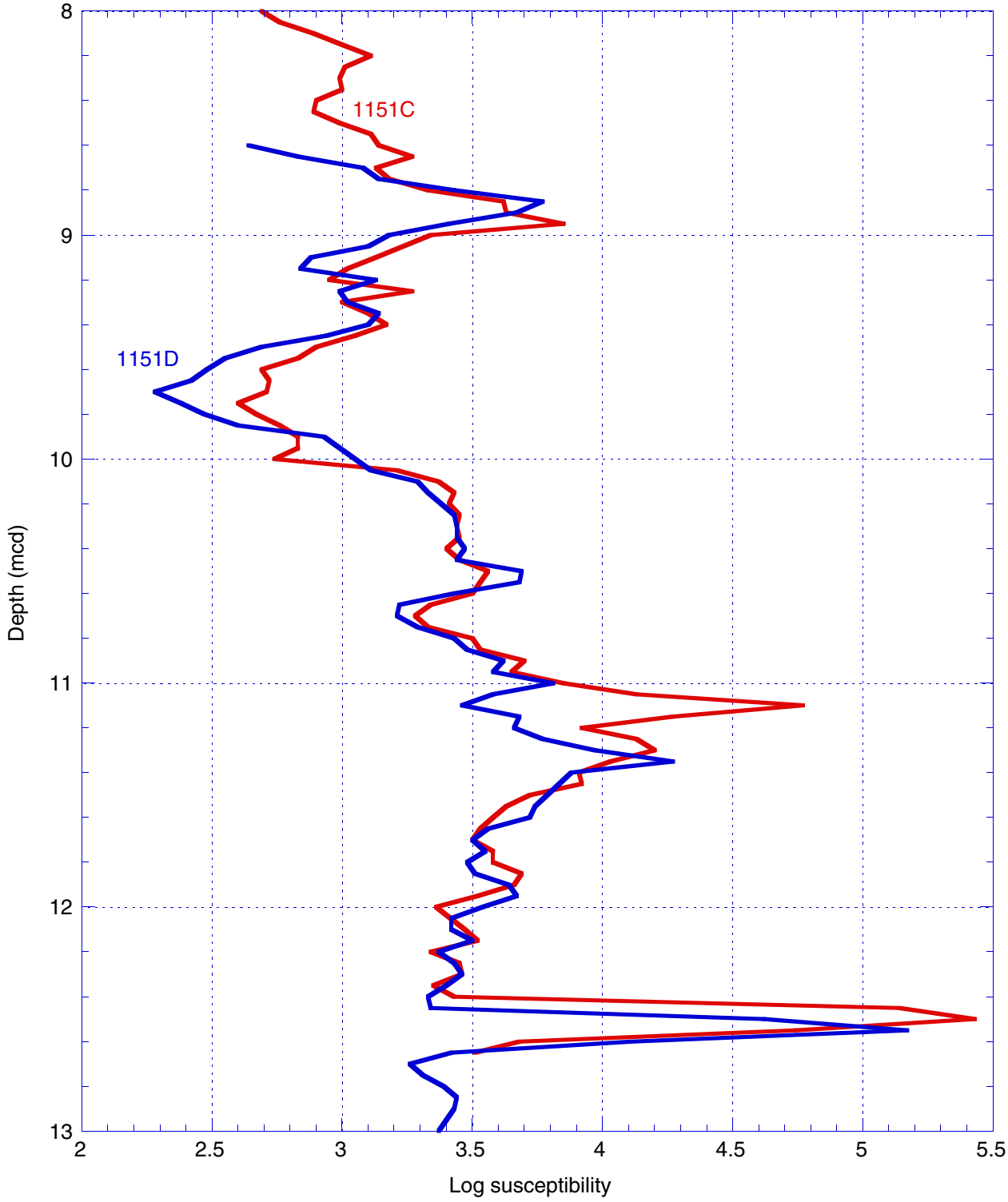

Table T1. Composite depth scale, Site 1151.

Core	Top depth (mbsf)	Top depth (mcd)	Offset (m)
186-1151A-			
1W*	0.0		
2R	78.0	80.13	2.13
3R	83.7	89.86	6.16
4R	93.3	99.79	6.49
5R	102.9	109.39	6.49
6R	112.6	119.09	6.49
7R	122.2	128.69	6.49
8R	131.8	138.29	6.49
9R	141.4	147.89	6.49
10R	151.0	157.49	6.49
1R	160.6	167.09	6.49
12R	170.2	176.69	6.49
13R	179.8	186.29	6.49
14R	189.5	195.99	6.49
15R	199.2	205.69	6.49
16R	208.9	215.39	6.49
17R	218.5	224.99	6.49
18R	228.1	234.59	6.49
19R†	237.7	244.19	6.49
20R	247.3	253.79	6.49
21R†	256.9	263.39	6.49
22R	266.6	273.09	6.49
23R	276.2	282.69	6.49
24R	285.9	292.39	6.49
25R	295.6	302.09	6.49
26R	305.3	311.79	6.49
27R	314.9	321.39	6.49
28R	324.6	331.09	6.49
29R	334.2	340.69	6.49
30R	343.9	350.39	6.49
31R	353.6	360.09	6.49
32R	363.2	369.69	6.49
33R	372.9	379.39	6.49
34R	382.5	388.99	6.49
35R	392.1	398.59	6.49
36R	401.4	407.89	6.49
37R	411.0	417.49	6.49
38R	420.6	427.09	6.49
39R	430.3	436.79	6.49
40R	439.9	446.39	6.49
41R	449.5	455.99	6.49
42R	459.2	465.69	6.49
43R	468.8	475.29	6.49
44R	478.4	484.89	6.49
45R	488.0	494.49	6.49
46R	497.6	504.09	6.49
47R	507.2	513.69	6.49
48R	516.8	523.29	6.49
49R	526.4	532.89	6.49
50R	536.0	542.49	6.49
51R	545.7	552.19	6.49
52R	555.4	561.89	6.49
53R	565.1	571.59	6.49
54R	574.7	581.19	6.49
55R	584.3	590.79	6.49
56R	593.9	600.39	6.49
57R	603.5	609.99	6.49
58R	613.2	619.69	6.49
59R	622.9	629.39	6.49
60R	632.5	638.99	6.49
61R	642.1	648.59	6.49
62R	651.6	658.09	6.49
63R	661.2	667.69	6.49
64R	670.8	677.29	6.49
65R	680.2	686.69	6.49
66R	689.8	696.29	6.49
67R	699.4	705.89	6.49
68R	709.0	715.49	6.49
69R	718.6	725.09	6.49
70R	728.3	734.79	6.49
71R	738.0	744.49	6.49
72R	747.7	754.19	6.49
73R	757.3	763.79	6.49
74R	766.9	773.39	6.49
75R	776.5	782.99	6.49
76R	786.1	792.59	6.49
77R	795.7	802.19	6.49
78R	805.4	811.89	6.49
79R	815.0	821.49	6.49
80R	824.6	831.09	6.49
81R	834.2	840.69	6.49
82R	843.8	850.29	6.49
83R	853.4	859.89	6.49
84R	863.1	869.59	6.49
85R	872.8	879.29	6.49
86R	882.3	888.79	6.49
87R	891.9	898.39	6.49
88R	901.6	908.09	6.49
89R	911.2	917.69	6.49
90R	920.8	927.29	6.49
91R	930.4	936.89	6.49
92R	940.1	946.59	6.49
93R	949.7	956.19	6.49
94R	959.3	965.79	6.49
95R	968.9	975.39	6.49
96R	978.6	985.09	6.49
97R	988.2	994.69	6.49
98R	997.8	1004.29	6.49
99R	1007.4	1013.89	6.49
100R	1017.0	1023.49	6.49
101R	1026.6	1033.09	6.49
102R	1036.2	1042.69	6.49
103R	1045.9	1052.39	6.49
104R	1055.6	1062.09	6.49
105R	1065.3	1071.79	6.49
106R	1075.0	1081.49	6.49
107R	1084.6	1091.09	6.49
108R	1094.3	1100.79	6.49
109R	1103.9	1110.39	6.49
186-1151C-			
1H	0.0	0.15	0.15
2H	2.2	3.05	0.85
3H	11.7	12.95	1.25
4H	21.2	22.59	1.39
5H	30.7	32.31	1.61
6H	40.2	41.86	1.66
7H	49.7	52.01	2.31
8H	59.2	62.21	3.01
9H	68.7	72.41	3.71
10H	78.2	82.26	4.06
11H	87.7	92.91	5.21
186-1151D-			
1H	0.0	0.00	0.00
2H	7.5	8.50	1.00
3H	17.0	18.60	1.60
4H	26.5	27.66	1.16
5H	36.0	35.71	–0.29
6H	45.5	45.16	–0.34
7H	55.0	55.61	0.61
8H	64.5	65.56	1.06
9H	74.0	76.16	2.16
10H	83.5	86.61	3.11

Notes: * = Core 186-1151A-1W is a wash core collected from the upper 78 m of Hole 1151A that was drilled rather than cored as part of a jet-in test. No depth adjustment is applied. † = the upper ~20 cm of these cores may be disturbed because Davis-Villinger Temperature Probe (DVTP) measurements were made after the collection of the preceding core. This table is also available in **ASCII.**

Table T2. Intervals disturbed or distorted by coring or whole-round sample collection.

Core	Section	Interval top* (cm)	Interval bottom* (cm)
186-1151A-			
2R	1	0	150
2R	2	0	50
3R	1	0	10
5R	1	0	75
6R	1	0	8
8R	1	0	8
8R	2	145	150
11R	2	145	150
14R	3	47	65
15R	1	0	20
20R	1	0	20
186-1151C-			
1H	1	0	15
1H	1	145	150
2H	1	0	15
2H	3	145	150
3H	1	0	8
3H	3	145	150
4H	1	0	35
5H	1	0	20
9H	1	0	10
9H	2	142	150
11H	1	0	15
11H	2	147	150
186-1151D-			
1H	1	0	25
1H	1	137	150
2H	1	0	10
4H	1	0	34
5H	1	0	15
5H	1	120	150
6H	1	0	10
7H	1	0	25
8H	1	0	20
9H	1	0	8
9H	3	146	150
10H	1	0	27

Notes: * = intervals listed above were not used in the construction of the meters composite depth scale (see "Data," p. 3). This table is also available in ASCII.

Table T3. Correlation of ash layers, Site 1151.

Feature	Data sets that correlate	Hole	Core	Section	Top interval (cm)	Depth (mcd)	Hole	Core	Section	Top interval (cm)	Depth (mcd)	Notes
Ash	Core photo, susceptibility, a*	C	2	7	36	12.41	D	2	3	99	12.49	Bioturbated ash with sharp base, possibly reworked†
Ash	Core photo	C	4	3	95	26.55	D	3	6	85	26.95	Ash layer distinct in Hole 1151D photo; thicker and more patchy in Hole 1151C photo, reworked†, correlation uncertain
Ash	Core photo, susceptibility	C	4	6	137	31.53	D	4	3	90	31.56	Ash layer underlain by dark silt in Hole 1151D, ash patch in Hole 1151C
Ash	Core photo, susceptibility	C	5	1	142	33.73	D	4	5	24	33.90	~7-cm-thick ash layer with double peak in susceptibility matching core above
Ash	Core photo	C	5	4	44	37.25	D	4	7	65	37.31	Biotite crystals common
Ash	Susceptibility	C	6	3	64	45.50	D	5-6				~8-cm-thick ash layer in Hole 1151C, but this layer is lost between Cores 5H and 6H in Hole 1151D; surrounding susceptibility correlates well
Ash	Core photo, susceptibility	C	7	1	124	53.25	D	6	6	56	53.22	Ash layer
Ash	Core photo, susceptibility, a*	C	7	4	80	57.31	D	7	2	17	57.28	Ash layer with sharp lower boundary and diffuse upper boundary (see Fig. **F3**, p. 12.)
Ash	Core photo, susceptibility, a*	C	7	4	116	57.67	D	7	2	54	57.65	Light colored ash, part of triple peak in susceptibility (see Fig. **F3**, p. 12).
Ash	Core photo	C	7	5	70	58.71	D	7	3	13	58.74	Light colored fine-grained ash layer (see Fig. **F3**, p. 12.)
Ash	Core photo, susceptibility	C	8	1	19	62.40	D	7	5	70	62.31	Bioturbated ash
Ash	Core photo, susceptibility, a*	C	8	7	18	71.39	D	8	5	4	71.60	Bioturbated ash layer, double peaks in susceptibility, correlation uncertain
Ash	Core photo, susceptibility	C	8	7	40	71.61	D	8	5	20	71.76	Bioturbated ash layer, correlation uncertain
Ash	Core photo	C	9	1	7	72.48	D	8	5	95	72.51	Ash layer
Ash	Core photo, susceptibility	C	9	1	137	73.78	D	8	6	73	73.79	Bioturbated ash layer, correlation uncertain
Ash	Core photo, susceptibility	C	9	2	104	74.95	D	8	7	43	74.99	Thin ash layer
Ash	Core photo, susceptibility	C	9	3	14	75.55	D	8	CC	7	75.52	Coarse-grained, dark ash layer with sharp base†
Ash	Core photo, susceptibility	C	9	4	136	78.27	D	9	2	55	78.21	Light ash patches
Ash	Core photo, susceptibility	C	9	5	140	79.81	D	9	3	66	79.82	~2-cm-thick ash layer in Hole 1151C, ash patch in Hole 1151D
Ash	Core photo, susceptibility	C	9	6	76	80.67	D	9	4	0	80.64	Bright white ash layers
Ash	Core photo, susceptibility	C	10	2	119	84.95	D	9	7	13	84.92	4- to 5-cm-thick ash with sharp base and irregular top correlates very well in susceptibility and photos
Ash	Core photo, susceptibility	C	10	4	117	87.93	D	10	1	93	87.54	Ash layer, correlation uncertain
Ash	Core photo, susceptibility	C	10	7	65	91.91	D	10	4	82	91.93	Fine ash layers with sharp bases and diffuse tops

Notes: † = **Aoki and Sakamoto** (this volume). Additional ash layers and patches are described in Table **T3** of **Aoki and Sakamoto** (this volume). This table is also available in **ASCII.**

Table T4. Splice tie points, Site 1151.

Core, section	Depth (mbsf)	Depth (mcd)		Core, section	Depth (mbsf)	Depth (mcd)
186-1151D-1H-3	3.80	3.80	Tie to	186-1151C-2H-1	2.95	3.80
186-1151C-2H-5	9.50	10.35	Tie to	186-1151D-2H-2	9.35	10.35
186-1151D-2H-6	15.40	16.40	Tie to	186-1151C-3H-3	15.15	16.40
186-1151C-3H-6	20.45	21.70	Tie to	186-1151D-3H-3	20.10	21.70
186-1151D-3H-4	22.95	24.55	Tie to	186-1151C-4H-2	23.16	24.55
186-1151C-4H-6	29.92	31.31	Tie to	186-1151D-4H-3	30.15	31.31
186-1151D-4H-7	35.70	36.86	Tie to	186-1151C-5H-4	35.25	36.86
186-1151C-5H-7	39.60	41.21	Tie to	186-1151D-5H-4	41.50	41.21
186-1151D-5H-7	45.25	44.96	Tie to	186-1151C-6H-3	43.30	44.96
186-1151C-6H-5	47.35	49.01	Tie to	186-1151D-6H-3	49.35	49.01
186-1151D-6H-6	54.25	53.91	Tie to	186-1151C-7H-2	51.60	53.91
186-1151C-7H-7	58.65	60.96	Tie to	186-1151D-7H-4	60.35	60.96
186-1151D-7H-6	63.30	63.91	Tie to	186-1151C-8H-2	60.90	63.91
186-1151C-8H-5	66.65	69.66	Tie to	186-1151D-8H-3	68.60	69.66
186-1151D-8H-5	71.80	72.86	Tie to	186-1151C-9H-1	69.15	72.86
186-1151C-9H-7	77.80	81.51	Tie to	186-1151D-9H-4	79.35	81.51
186-1151D-9H-6	82.45	84.61	Tie to	186-1151C-10H-2	80.55	84.61
186-1151C-10H-7	87.85	91.91	Tie to	186-1151D-10H-4	88.80	91.91
186-1151D-10H-7	93.00	96.11	Tie to	186-1151C-11H-3	90.90	96.11
186-1151C-11H-7	97.20	102.41	Tie to	186-1151A-4R-2	95.92	102.41
186-1151A-4R-5	99.35	105.84				

Note: This table is also available in **ASCII.**